JACS
JOURNAL OF THE AMERICAN CHEMICAL SOCIETY
Article
Cite This: J. Am. Chem. Soc. 2018, 140, 16206−16212
pubs.acs.org/JACS

Ferromagnetism of 1T′-MoS_2 Nanoribbons Stabilized by Edge Reconstruction and Its Periodic Variation on Nanoribbons Width

Kaiyun Chen,[†] Junkai Deng,[*,†] Xiangdong Ding,[†] Jun Sun,[†] Sen Yang,[*,†] and Jefferson Zhe Liu[*,‡]

[†]MOE Key Laboratory for Nonequilibrium Synthesis and Modulation of Condensed Matter, State Key Laboratory for Mechanical Behavior of Materials, Xi'an Jiaotong University, Xi'an 710049, China

[‡]Department of Mechanical Engineering, The University of Melbourne, Parkville, Victoria 3010, Australia

Supporting Information

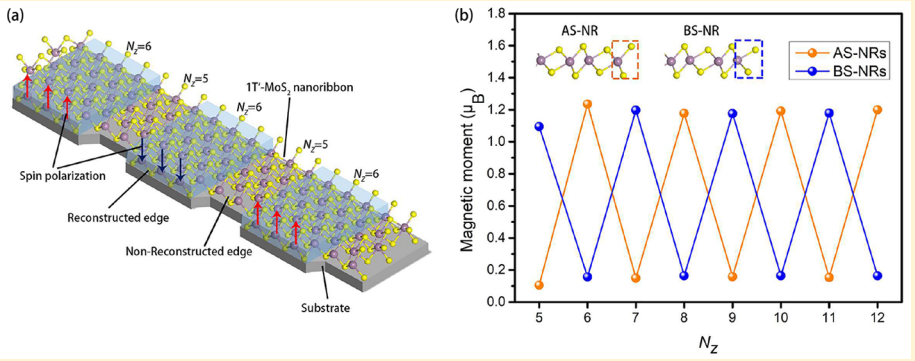

ABSTRACT: Nanoribbons (NRs) of two-dimensional (2D) materials have attracted intensive research interests because of exotic physical properties at edges as well as tunable properties via width control. In this paper, using density functional theory (DFT) calculations, we discover sensitive dependence of magnetic properties of 1T′-MoS_2 NRs, that is, periodic variation of magnetic moments between 0.1 and 1.2 μ_B, on NR width (even or odd number of MoS_2 units). Our results reveal that a special edge reconstruction, which is not recognized before, stabilizes the ferromagnetic (FM) ground state. Our results also suggest that the FM state could be stable under ambient condition. This study indicates a promising means to integrate multiple magnetic units for small-scale functional devices, such as information storage and spintronics, on a single piece of MoS_2 NR by designing segments with different width.

1. INTRODUCTION

Two-dimensional (2D) transition metal dichalcogenides (TMDs) exhibit a combination of atomic thin crystal structure, direct band gap, strong spin−orbit coupling, and robust yet flexible mechanical property.[1−4] They have attracted intensive research interests in fundamental studies and practical applications for flexible electronic, optoelectronic, spintronic, catalysts, piezoelectricity, and energy harvesting.[5−13] Molybdenum disulfide (MoS_2) is the mostly studied TMD. It has three crystal phases, 2H, 1T, and 1T′.[14,15] The most studied 2H phase is a semiconductor with a direct bandgap of 1.9 eV. The 1T phase is metallic and metastable.[16,17] It usually undergoes a periodic structural distortion for Mo "dimerization", leading to the 1T′ phase (Figure 1 and Figure S1). The 1T′ phase can be stabilized under appropriate thermal or chemical conditions.[18−20]

When tailoring 2H-TMD in the form of nanoribbons (NRs), nanoclusters, or nanoflakes, the exposed edges often exhibit distinctive properties from its bulk form.[21−24] Zhen Zhou et al. reported that the zigzag edges of semiconductor 2D TMD NRs become metallic,[21] owing to the appearance of edge states in the bulk band gap. Moreover, it has been predicted these edge states could be ferromagnetic.[21,24,25] The presence of edge states gives rise to an enhanced photoluminescence response, an extraordinary catalytic behavior both in hydrodesulfurization and hydrogen evolution reaction, spintronics, and unusual 1D plasmonic excitation.[26−30] The as-cut edges usually are accompanied by excess unpaired electrons known as dangling bonds, rendering the system energetically unstable. They will undergo reconstruction to passivate the dangling bonds. The reconstructed edge structures determine the interesting properties mentioned above. Different types of reconstruction lead to distinctive electronic properties.[31] It is essential to uncover the likely edge reconstruction and to explore the potentially exotic physical or chemical properties.

Compared with the mostly studied 2H phase, 1T′-MoS_2 has a more complex crystal structure and chemical bonds. The 2H phase has one MoS_2 unit in primitive cell and one type of Mo−S covalent bond (2.41 Å). The distorted 1T′ phase has two MoS_2 units in primitive cell and four different Mo−S bond length (2.42 Å, 2.39 Å, 2.48 and 2.51 Å) as well as the Mo

Received: August 28, 2018
Published: November 9, 2018

DOI: 10.1021/jacs.8b09247
J. Am. Chem. Soc. 2018, 140, 16206−16212

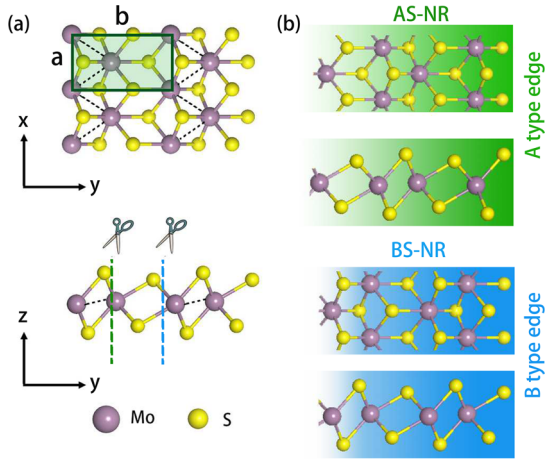

Figure 1. Two types of zigzag 1T′-MoS_2 nanoribbons. (a) Top and front views of pristine 1T′-MoS_2 monolayer crystal. The Mo−Mo "dimers" are drawn as black dot lines. (b) Two types of 1T′ zigzag nanoribbons according to two different structures at the S edges. They are named as AS-NRs and BS-NRs, respectively. The width of nanoribbon (N_Z) is defined as the number of MoS_2 unit across the nanoribbon.

"dimer" bonds. It is likely to have more edge structures and reconstruction possibility in 1T′-MoS_2 NRs, implying more opportunities to uncover new and interesting physical properties.

In this paper, we employ density functional theory (DFT) calculations to investigate structure reconstruction and physical properties at zigzag edges of 1T′-MoS_2 NRs. At Mo edge, we reveal a previously unrecognized but energetically favorable reconstruction arising from charge transfer from Mo atoms to the weaker Mo−S bonds next to the edges. The reconstruction leads to a ferromagnetic (FM) ground state. Interestingly, the occurrence of edge reconstruction sensitively depends on NR width, for example, even or odd number of MoS_2 units, termed as "magic number". The magnetic moment consequently exhibits a periodic oscillation between 0.1 and 1.2 μ_B with the increase of NR width. This novel property could stimulate further study to integrate high density of spintronic or information storage units/devices in a single piece of 1T′-MoS_2 NR via width control.

2. RESULTS AND DISCUSSION

A single layer 1T′-MoS_2 can be regarded as a distorted form of 1T-MoS_2 (Figure S1a), where two adjacent rows of Mo atoms along the zigzag direction dimerize to form a zigzag chain, as depicted in Figure 1a. The Mo−Mo "dimer" has a bond length of 2.77 Å, which is much shorter than the Mo−Mo "nondimer" interatomic distance of 3.79 Å. The dimerization of 1T′-MoS_2 can be clearly demonstrated by electron local function (ELF) calculation shown in Figure S1b. The formation of such Mo−Mo "dimer" chains distorts the crystal, showing alternation of two different rhomboid units with one unit elongated in the thickness direction.

Previous studies concluded that zigzag edges are more energetic favorable for 2H-MoS_2 than the armchair counterparts. Accordingly, we generated the zigzag 1T′-MoS_2 NRs, following previous theoretical and experimental studies.[21,23−25] As shown in Figure 1b, there are two types of S atom terminated edges (S edges). The first type has a larger S−Mo−S angle, 80.78° (named as AS-NRs), and the second type has a smaller S−Mo−S angle, 70.93° (named as BS-NRs). We consider bare Mo edges in the other end of NRs, in light of the direct experimental observations in 2H-MoS_2 NRs.[24,25] The width N_Z is defined as the numbers of Mo atoms in the cross-section, which is consistent to the definition of 2H-MoS_2 NRs in previous studies.

The as-cut nanoribbons were fully relaxed in DFT calculations. Figure 2 shows the relaxed crystal structures of AS-NRs and BS-NRs with N_Z from 5 to 12. Some new edge structures at Mo-terminated edges (highlighted by red dashed boxes) can be observed in AS-NRs with even N_Z and BS-NRs with odd N_Z. The key structure feature is the two adjacent elongated rhomboid units at Mo edges. The Mo edge atoms have significant inward displacement toward the adjacent Mo atoms after relaxation, which appears like a "trimer-like" structure, and the energy reduction is ~1.27 eV. The Mo−Mo interatomic distance reduces from 3.79 to 2.95 Å, close to that of Mo−Mo "dimer" (2.77 Å) in pristine 1T′-MoS_2 (Figure 1a).

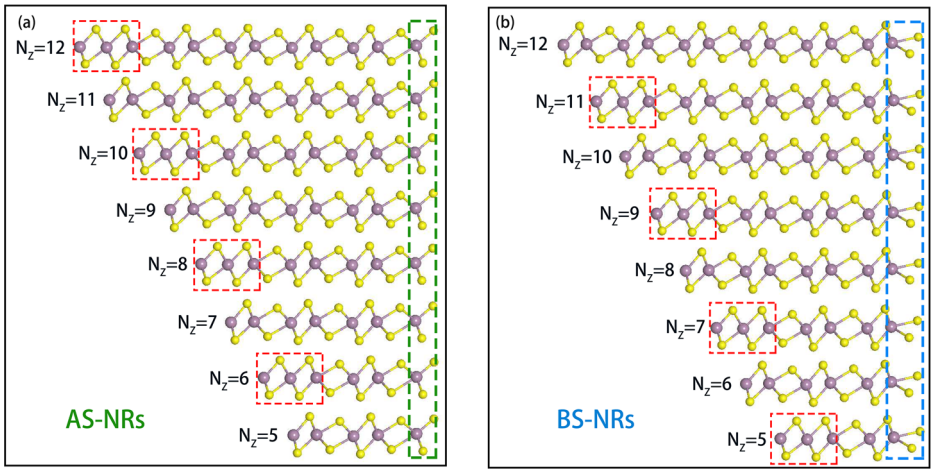

Figure 2. Reconstruction at Mo edges of the 1T′-MoS_2 nanoribbons. (a) Reconstructed Mo edges for AS-NRs. The edge reconstruction, which is highlighted by red dashed boxes, takes place at even N_Z, for example, 6, 8, 10, and 12. (b) In the case of BS-NRs, the reconstruction happens at odd N_Z, for example, 5, 7, 9, and 11. The key reconstruction feature is the two adjacent vertically elongated rhomboid units at the edge. No obvious edge structure change is observed in the S edges.

DOI: 10.1021/jacs.8b09247
J. Am. Chem. Soc. 2018, 140, 16206−16212

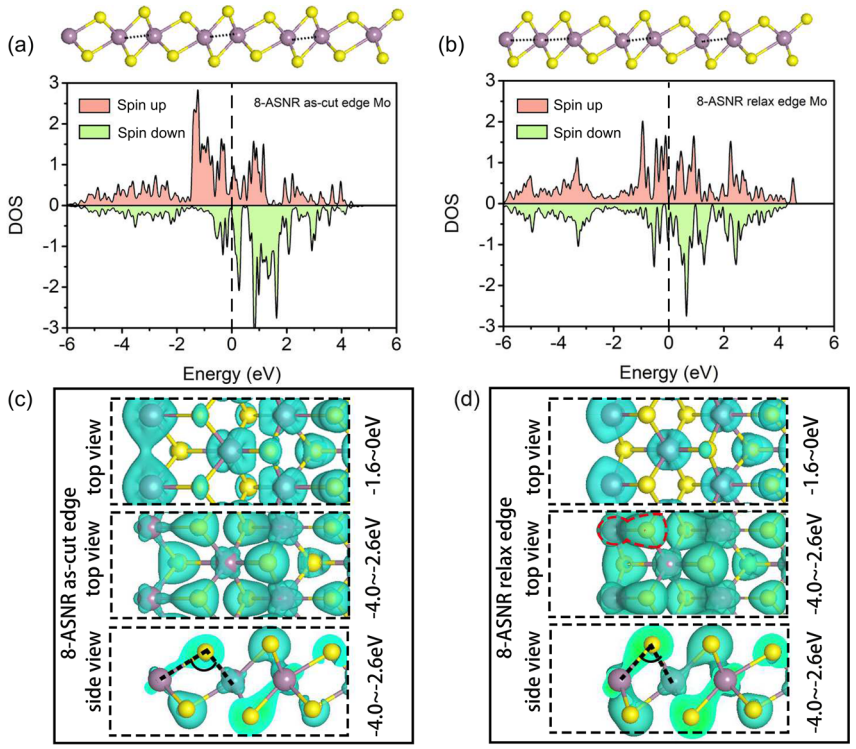

Figure 3. Physical origins of the Mo edge reconstruction. (a) Electron projection density of states (PDOS) of Mo atoms at the as-cut edges of AS-NRs with N_Z = 8. (b) PDOS of Mo atoms at the reconstructed edge of AS-NRs with N_Z = 8. (c) (d) Electron density distribution of as-cut and relaxed 8-ASNRs within different energy ranges with reference to Fermi level. The PDOS results indicate a strong electron transfer from (−1.6, 0) eV to lower energy level region as a result of edge reconstruction. Corresponding electrons are transferred from edge Mo atoms to the neighboring Mo−S bonds in panel d. The excess electron at this bond will cause a repulsion from the lone pair electron cloud on top of the S atoms. As a result, this Mo−S bond will rotate to reduce the Mo−S−Mo bond angle (from 99.22° to 76.61°), causing the edge Mo atoms moving inward.

For other cases, there is no obvious change of edge rhomboid units after relaxation. The Mo edge atoms just show a minor inward displacement, that is, Mo−Mo interatomic distance changing from 2.77 Å to ∼2.67 Å. Note that for all NRs, the S edges have no notable structural change after relaxation. We tried to artificially construct the "trimer-like" structures at S-terminated edge. After fully relaxation in our DFT calculations, those "trimer-like" S-terminated edges would spontaneously recover back to the original structure. The observed Mo edge reconstruction has not been reported in TMD NRs. In addition, such sensitive dependence of edge reconstruction on NR width (even or odd N_Z) is not observed in other 2D materials.

To reveal physical origin of the observed edge reconstruction, we study the electronic structure of 1T′-MoS_2 NRs. Figure 3 shows crystal structure and electronic structure of the as-cut and relaxed AS-NRs (N_Z = 8). The edge cutting breaks three Mo−S bonds and two Mo−Mo "dimer" bonds at the Mo edge. In addition, our Bader analysis (Table S1 and Figure S2) indicates about 0.25 electron being transferred from the S edge to the Mo edge. Polarization discontinuity in the as-cut NR generates a negatively charged S edge and a positively charged Mo edge, driving electrons transfer across the NR. Consequently, there will be significant unpaired electrons at bare Mo-edges in the as-cut NRs. They generate a significant magnetic moment 2.2 μ_B. In the projected electron density of state (PDOS), these unpaired electrons are located in energy level range (−1.6, 0) eV below the Fermi level (Figure 3a).

To reduce system total energy, these NRs should undergo edge structure reconstruction to self-passivate the unpaired electrons. Analogous to the Mo "dimerization" in 1T′ phase, it is natural to expect that the edge Mo atoms might move inward to "dimerize" with Mo atoms next to the edge, thus forming the "trimer-like" structure. It appears to be consistent to crystal structure change in Figure 2 and Figure 3b: the Mo−Mo interatomic distance of 2.95 Å close to that of Mo "dimer" 2.77 Å. However, our calculated electronic structure indicates a different physical origin. In pristine 1T′-MoS_2, energy levels of Mo "dimer" bonds are located in (−1.6, 0) eV range from the Fermi level (Figure S3), which overlaps that of the unpaired electrons in the as-cut NR (Figure 3a). Thus, Mo "dimer/trimer" is unlikely to reduce system total energy. Instead, via comparing Figure 3a and b, we observe significant charge transfer to the lower energy levels upon reconstruction. Figure 3c and d show the partial charge density within (−1.6, 0) eV and (−4.0, −2.6) eV ranges. There is no Mo "dimer" charge density between Mo atoms in edge region, distinctive from those in pristine 1T′-MoS_2 (Figure 3c and d the partial charge density, corresponding to the (−4.0, −2.6) eV energy level range, accumulates at the Mo−S bonds next to Mo edge atoms. This Mo−S bond in the as-cut NR has the longest bond length among all Mo−S bonds. It is thus reasonable for the charge transferring to this weaker bond. The excess charges in this bond would be repelled by the lone pair electrons on the top of S atom (Figure 3c), leading to a reduction of Mo−S−Mo bond angles and thus the inward motion of Mo edge atoms, forming the "trimer-like" edge structure.

For AS-NRs with an odd N_Z and BS-NRs with an even N_Z, the edge Mo atoms have "dimer" bonds with the adjacent Mo atoms. There is no possibility for the significant structure

DOI: 10.1021/jacs.8b09247
J. Am. Chem. Soc. 2018, 140, 16206−16212

change as discussed above. Nonetheless, electrons of the dangling bonds would redistribute, leading to small but observable inward displacement of Mo atom (i.e., reduction of Mo−Mo bond length from 2.77 to 2.67 Å).

Our DFT results conclude that the edge reconstruction stabilizes a ferromagnetic (FM) ground state in 1T′-MoS_2 NRs. Figure 4 shows the spin charge distribution and relative

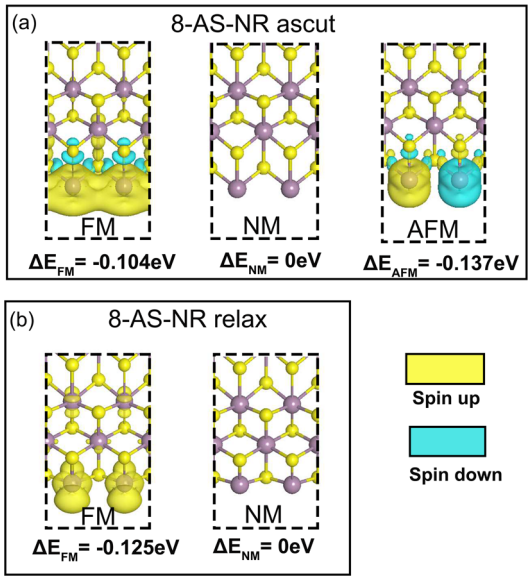

Figure 4. Edge reconstruction stabilizing FM state at Mo edges. (a) Spin charge distribution and relative total energy of the as-cut AS-NRs (N_Z = 8) with the FM, NM, and AFM states at the Mo edge. (b) Spin charge distribution and relative total energy results after the reconstruction. The relative total energy is defined with reference to the NM states. The AFM is the ground state in the as-cut NR. However, it is unstable after the edge reconstruction. Thus, edge reconstruction stabilizes FM state compared with NM and AFM.

total energy results of FM, antiferromagnetic (AFM), and nonmagnetic (NM) states for the case of AS-NR (N_Z = 8). The relative total energy (ΔE) is defined with reference to the NM state. The spin charge density is always localized at the Mo edge. In the case of as-cut NR, AFM is the ground state (Figure 4a). After edge reconstruction, the AFM state disappears. The FM becomes the ground state. It is total energy is −0.125 eV lower than that of NM state. This value significantly higher than thermal excitation energy of 0.026 eV at room temperature. From a 1D Ising model that only considers the nearest neighbor interaction, the Curie temperature could be predicted as high as ∼600 K. The FM state could be stable at ambient conditions, which is critical for applications based on magnetism. The magnetic moment of this NR is about 1.2 μ_B, smaller than 2.2 μ_B of the as-cut NR. Nonetheless, it is sufficient for practical applications.

In the past few years, there are significant experimental advances for characterizing the atomistic edge structures of MoS_2.[23−25,32−36] In some experiments, the bare Mo edges have been observed,[24,25,32,33] whereas other investigations found passivation of Mo edges by S or other atoms.[23,34−36] These experimental studies indicate that under appropriate conditions, the bare Mo edges can be fabricated in experiments. It is worth noting that recently, Zhao et al. have successfully grown wafer scale nanoporous 2D MoS_2 films.[25] They observed a new type of edge reconstruction, that is, "distorted 1T edge", in which 1T like crystal structure formed at the edges of 2H MoS_2. This edge structure bears some resemblance to those in Figure 2, despite that our MoS_2 NRs are in 1T′ phase. The interesting observation in Zhao's experimental work and our DFT study suggests rich physics of the edges of TMD materials that remains to be explored.

In practice, the 2D NRs should be supported by some substrates. It is probable that the structure and physical properties of NR edges could be affected by the substrates. Indeed, Xu et al.[34] and Cheng et al.[35] observed that the MoS_2 nanowire edges would interact with Au substrates to form some 1D superstructures. To examine this effect, we performed further DFT calculations to study the edge reconstruction of 1T′ NRs on top of 2H MoS_2 substrates. We find that the substrates have negligible effects on the observed edge reconstruction (Figure 2) and magnetic properties (Figure 4). It is reasonable since there are only weak van der Waals and Coulomb interactions between the MoS_2 layers, and thus, negligible interlayer charge transfer is observed (Figure S4 and Table S2).

We would also like to point out that recently Luxa and Sofer et al. detected room temperature ferromagnetic ordering of layered MoS_2 in 1T′ phase.[37] The authors attributed the ferromagnetism to the edges. This experiment might provide an indirect evidence to support our DFT calculation results.

Figure 5 summarizes the magnetic moments, lattice constants, and binding energy results of NRs as a function of different N_Z. It shows that the magnetic moment sensitively depends on N_Z. The AS-NRs with edge reconstruction (even N_Z) have a larger magnetic moment about 1.2 μ_B. For the rest of AS-NRs (odd N_Z), they have a much smaller value 0.1 μ_B. A similar conclusion can be drawn for BS-NRs. Therefore, the magnetic moment exhibits an interesting periodic oscillation as N_Z changes. The lattice constant a_x (along the longitudinal direction) and binding energy E_b also show a periodic variation with respect to N_Z in Figure 5b and c. Clearly, such a periodic variation is a result of the edge reconstruction. As N_Z increases, a_x converges to the value of pristine 1T′-MoS_2 crystal in Figure 5b. The edge effect on lattice constant diminishes when N_Z is large enough. The binding energy is defined as

$$E_b = \frac{nE(\mathrm{Mo}) + mE(\mathrm{S}) - E(\mathrm{Mo}_n\mathrm{S}_m)}{n + m} \quad (1)$$

where E(Mo), E(S) and $E(\mathrm{Mo}_n\mathrm{S}_m)$ are the total energy of Mo atom, S atom and $\mathrm{Mo}_n\mathrm{S}_m$ crystal, n and m are the number of atoms, respectively. A higher E_b value represents a stabler structure. In Figure 5c, a narrower NR has a lower E_b, arising from a higher portion of edges in the crystal. We observe two bounds for E_b. The upper bound corresponds to NRs without edge reconstruction and the lower bound is for NRs with edge reconstruction. Because edge reconstruction take place at either odd or even N_Z, E_b exhibits a stairstep-wise variation enclosed by these two bounds.

In Figure 5c, comparing the two types of NRs with the same N_Z, we find that the one with a stronger magnetic moment always has a smaller E_b value. For example, at N_Z = 8, the AS-NR has E_b = 4.782 eV and μ = 1.17 μ_B, while BS-NR has E_b = 4.793 eV and μ = 0.16 μ_B. To examine the stability of the stronger FM state, we performed climbing image nudged elastic band (NEB) calculations for AS-NR (N_Z = 8) and BS-NR (N_Z = 7). The results are summarized in Figures S5 and S6. We gradually move the two adjacent elongated rhomboid units from the Mo edge to the S edge. The energy barrier is as

DOI: 10.1021/jacs.8b09247
J. Am. Chem. Soc. 2018, 140, 16206−16212

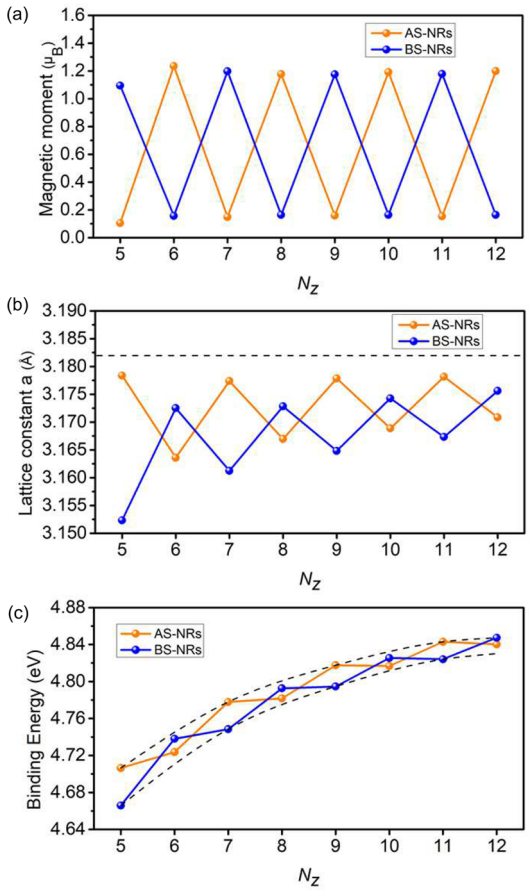

Figure 5. Sensitive dependence of magnetic, structure, and energetic properties on N_Z (even or odd), the so-called magic number. (a) Periodic variation of magnetic moments of 1T′-MoS_2 NRs as a function of N_Z. The AS-NRs with an even number of N_Z has a larger magnetic moment, 1.2 μ_B. In contrast, the BS-NRs with an odd number of N_Z has a larger magnetic moment of similar magnitude. (b) Lattice constant a_x also exhibits a similar periodic oscillation as a function of N_Z. The black dashed line denotes the lattice constant of pristine 1T′-MoS_2. (c) Binding energy of 1T′-MoS_2 NRs exhibits a periodic variation enclosed by two bounds.

high as ∼500 meV, indicating the stability of the NRs with high magnetic moment under ambient condition.

It is known that geometry of a nanostructure, such as NRs, nanotubes, nanoholes, etc., significantly affect its physical properties. For a graphene armchair NR, its band gap sensitively depends on its width N_Z = 3p−1,3p or 3p+1 (where "p" is a positive integer number) when periodic holes are induced to it.[38] The armchair ZrS_2 NRs has a nearly constant band gap at an odd N_Z, but a significant increased band gap with N_Z reduction.[39] ZnS single wall nanotube of (3n, 0) (n is a positive integer number) has the highest stability and largest band gap among others.[40] Such special structure parameter is often called as magic number. There are rare reports for magic number related to magnetic properties. Our result (Figure 5a) is a new phonemenon.

Inspired by our discovery, it seems feasible to integrate multiple magnetic units into a single piece of MoS_2 NR. We could create a single piece of AS-NR/BS-NR composed of segments with different widths, for example, segments with even (odd) N_Z (high magnetic moments) separated by segments with odd (even) N_Z (low magnetic moments) as shown in Figure 6a. If the two types of segments maintain the

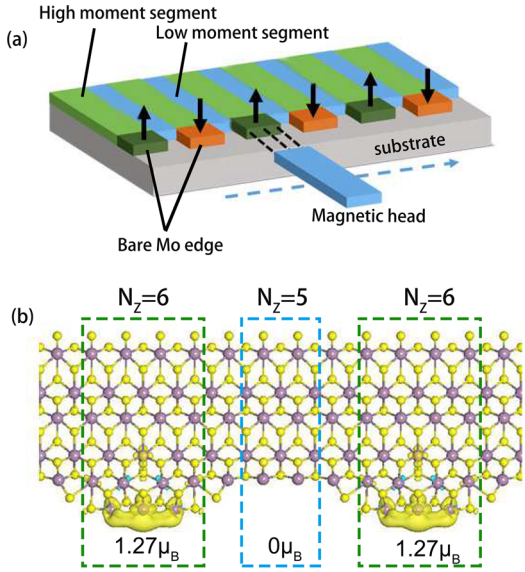

Figure 6. (a) Prototype of information storage device made of a single piece of MoS_2 NR, which composes of segments with different N_Z (high or low magnetic moment). The black arrows respresent the spin polarization direction. (b) Spin charge distribution of AS-NR supercell with three-units of N_Z = 6 (high magnetic moment) and two-units of N_Z = 5 (low magnetic moment) segments. FM is confirmed as ground state. As expected high magnetic moment occurs at N_Z = 6 segments.

magnetic moments, in principle, we could use local external magnetic field to separately manipulate spin-up or spin-down state of each high magnetic moment segment without interference. A protypical model is examined. Figure 6b shows a AS-NR supercell including alternated segments with N_Z = 6 (three units) and N_Z = 5 (two units). The FM state is confirmed to be ground state. As expected, the magnetic moments (1.27 μ_B) mainly concentrate on the edge of N_Z = 6 segment, which is close to the infinite long AS-NR of N_Z = 6 (Figure 5a). The segment with N_Z = 5 has nearly zero μ_B. Controllable fabrication of MoS_2 NRs or flakes has significantly advanced in past few years. It is reasonable to expect in near future we can fabricate NRs with precisely controlled N_Z. In addition, it has been observed that the MoS_2 NR edges are not straight.[32,33] The alternative variation of N_Z naturally exits in experiment, implying the fessibility of our prototype. This prototypical model suggests a great potential to fabricate high density integrated magnetic devices for information storage and spintronics applications.

3. CONCLUSION

In this paper, using DFT calculations, we investigate the edge reconstruction of 1T′-MoS_2 NRs and the related physical properties. We find a new type of edge reconstruction taking place at some specific width N_Z, that is, even N_Z for AS-NR and odd N_Z BS-NRs. The edge reconstruction stabilizes the FM state with a magnetic moment of 1.2 μ_B. This FM state could be stable at ambient condition. With the increasing of N_Z, the magnetic moment periodically oscillates between 0.1 μ_B and 1.2 μ_B. Such sensitive dependence of magnetic property on NR width could open new opportunities for information storage and spintronic applications in a single piece of 1T′-MoS_2 NR.

DOI: 10.1021/jacs.8b09247
J. Am. Chem. Soc. 2018, 140, 16206−16212

4. COMPUTATIONAL METHODS

Our DFT calculations were conducted by using the Vienna Ab-inito Simulation Package (VASP).[41] The spin polarized Perdew–Burke–Ernzerhof (PBE) exchange-correlation functional[42] and projector augmented wave method[43] were adopted. The cutoff energy of 400 eV and the Monkhorst–Pack k-point mesh[44] of 15 × 1 × 1 for 1T′-MoS_2 unit cell were used to ensure that atomic positions and lattice constants were fully relaxed until total energy difference and forces were less than 10^{-5} eV and 0.01 eV/Å, respectively. A higher convergence criterion for total energy, 10^{-6} eV, was adopted to calculate electronic structures. Periodic boundary condition was applied in all three directions. A vacuum space of at least 20 Å was applied in y and z directions to avoid the interaction between a NR and its periodic images. The nudged elastic band (NEB) method[45] was employed to study migration of Mo "trimer" from edge to interior of MoS_2 nanoribbons.

■ ASSOCIATED CONTENT

Supporting Information

The Supporting Information is available free of charge via the Internet at http://pubs.acs.org/. The Supporting Information is available free of charge on the ACS Publications website at DOI: 10.1021/jacs.8b09247.

Electron local function, charge analysis, and electron structure of pristine 1T′-MoS_2, relative energy of "trimer", migration energy "trimer" of 1T′′-MoS_2 nanoribbons, all supplemental figures (PDF)

■ AUTHOR INFORMATION

Corresponding Authors

*junkai.deng@mail.xjtu.edu.cn
*yangsen@mail.xjtu.edu.cn
*zhe.liu@unimelb.edu.au

ORCID

Junkai Deng: 0000-0001-6288-4241
Jefferson Zhe Liu: 0000-0002-5282-7945

Notes

The authors declare no competing financial interest.

■ ACKNOWLEDGMENTS

The authors gratefully acknowledge the support of NSFC (Grants Nos. 51728203, 51471126, 51320105014, 51621063) and the support by 111 project 2.0 (Grant No. BP2018008). J.D. also thanks the support of the China Postdoctoral Science Foundation (Grant No. 2016T90911) and the Fundamental Research Funds for the Central Universities. J.Z.L. acknowledges the support from ARC discovery projects and HPC from National Computational Infrastructure from Australia. This work is also supported by State Key Laboratory for Mechanical Behavior of Materials and HPC platform of Xi'an Jiaotong University.

■ REFERENCES

(1) Lebègue, S.; Eriksson, O. Electronic structure of two-dimensional crystals from ab initio theory. *Phys. Rev. B: Condens. Matter Mater. Phys.* **2009**, *79*, 115409.

(2) Li, W.; Li, J. Ferroelasticity and domain physics in two-dimensional transition metal dichalcogenide monolayers. *Nat. Commun.* **2016**, *7*, 10843.

(3) Duerloo, K.-A. N.; Ong, M. T.; Reed, E. J. Intrinsic Piezoelectricity in Two-Dimensional Materials. *J. Phys. Chem. Lett.* **2012**, *3*, 2871.

(4) Shirodkar, S. N.; Waghmare, U. V. Emergence of ferroelectricity at a metal-semiconductor transition in a 1T monolayer of MoS_2. *Phys. Rev. Lett.* **2014**, *112*, 157601.

(5) Acerce, M.; Voiry, D.; Chhowalla, M. Metallic 1T phase MoS_2 nanosheets as supercapacitor electrode materials. *Nat. Nanotechnol.* **2015**, *10*, 313.

(6) Ramasubramaniam, A.; Naveh, D. Mn-doped monolayer MoS_2: An atomically thin dilute magnetic semiconductor. *Phys. Rev. B: Condens. Matter Mater. Phys.* **2013**, *87*, 195201.

(7) Zhao, C.; et al. Enhanced valley splitting in monolayer WSe_2 due to magnetic exchange field. *Nat. Nanotechnol.* **2017**, *12*, 757.

(8) Xiao, J.; Choi, D.; Cosimbescu, L.; Koech, P.; Liu, J.; Lemmon, J. P. Exfoliated MoS_2 Nanocomposite as an Anode Material for Lithium Ion Batteries. *Chem. Mater.* **2010**, *22*, 4522.

(9) Wang, D.; Liu, L. M.; Zhao, S. J.; Hu, Z. Y.; Liu, H. Potential Application of Metal Dichalcogenides Double-Layered Heterostructures as Anode Materials for Li-Ion Batteries. *J. Phys. Chem. C* **2016**, *120*, 4779.

(10) Radisavljevic, B.; Radenovic, A.; Brivio, J.; Giacometti, V.; Kis, A. Single-layer MoS_2 transistors. *Nat. Nanotechnol.* **2011**, *6*, 147.

(11) He, J.; Hummer, K.; Franchini, C. Stacking effects on the electronic and optical properties of bilayer transition metal dichalcogenides MoS_2, $MoSe_2$, WS_2, and WSe_2. *Phys. Rev. B: Condens. Matter Mater. Phys.* **2014**, *89*, 075409.

(12) Yoder, M. A.; Yan, Z.; Han, M.; Rogers, J. A.; Nuzzo, R. G. Semiconductor Nanomembrane Materials for High-Performance Soft Electronic Devices. *J. Am. Chem. Soc.* **2018**, *140*, 9001.

(13) Chou, S. S.; Sai, N.; Lu, P.; Coker, E. N.; Liu, S.; Artyushkova, K.; Luk, T. S.; Kaehr, B.; Brinker, C. J. Understanding catalysis in a multiphasic two-dimensional transition metal dichalcogenide. *Nat. Commun.* **2015**, *6*, 8311.

(14) Zhu, J.; Wang, Z.; Yu, H.; Li, N.; Zhang, J.; Meng, J.; Liao, M.; Zhao, J.; Lu, X.; Du, L.; Yang, R.; Shi, D.; Jiang, Y.; Zhang, G. Argon plasma induced phase transition in monolayer MoS_2. *J. Am. Chem. Soc.* **2017**, *139*, 10216.

(15) Tan, S. J. R.; Abdelwahab, I.; Ding, Z.; Zhao, X.; Yang, T.; Loke, G. Z. J.; Lin, H.; Verzhbitskiy, I.; Poh, S. M.; Xu, H.; Nai, C. T.; Zhou, W.; Eda, G.; Jia, B.; Loh, K. P. Chemical stabilization of 1T′ phase transition metal dichalcogenides with giant optical kerr nonlinearity. *J. Am. Chem. Soc.* **2017**, *139*, 2504.

(16) Kan, M.; Wang, J. Y.; Li, X. W.; Zhang, S. H.; Li, Y. W.; Kawazoe, Y.; Sun, Q.; Jena, P. Structures and Phase Transition of a MoS_2 Monolayer. *J. Phys. Chem. C* **2014**, *118*, 1515.

(17) Duerloo, K. A.; Li, Y.; Reed, E. J. Structural phase transitions in two-dimensional Mo- and W-dichalcogenide monolayers. *Nat. Commun.* **2014**, *5*, 4214.

(18) Zhuang, H. L.; Johannes, M. D.; Singh, A. K.; Hennig, R. G. Doping-controlled phase transitions in single-layer MoS_2. *Phys. Rev. B: Condens. Matter Mater. Phys.* **2017**, *96*, 165305.

(19) Kang, Y.; Najmaei, S.; Liu, Z.; Bao, Y.; Wang, Y.; Zhu, X.; Halas, N. J.; Nordlander, P.; Ajayan, P. M.; Lou, J.; Fang, Z. Plasmonic hot electron induced structural phase transition in a MoS_2 monolayer. *Adv. Mater.* **2014**, *26*, 6467.

(20) Duerloo, K. A.; Reed, E. J. Structural Phase Transitions by Design in Monolayer Alloys. *ACS Nano* **2016**, *10*, 289.

(21) Li, Y.; Zhou, Z.; Zhang, S.; Chen, Z. MoS_2 Nanoribbons: High Stability and Unusual Electronic and Magnetic Properties. *J. Am. Chem. Soc.* **2008**, *130*, 16739.

(22) Bollinger, M. V.; Lauritsen, J. V.; Jacobsen, K. W.; Norskov, J. K.; Helveg, S.; Besenbacher, F. One-dimensional metallic edge states in MoS_2. *Phys. Rev. Lett.* **2001**, *87*, 196803.

(23) Zhou, W.; Zou, X.; Najmaei, S.; Liu, Z.; Shi, Y.; Kong, J.; Lou, J.; Ajayan, P. M.; Yakobson, B. I.; Idrobo, J. C. Intrinsic structural defects in monolayer molybdenum disulfide. *Nano Lett.* **2013**, *13*, 2615.

(24) Zhang, J.; Soon, J. M.; Loh, K. P.; Yin, J.; Ding, J.; Sullivian, M. B.; Wu, P. Magnetic Molybdenum Disulfide Nanosheet Films. *Nano Lett.* **2007**, *7*, 2370.

DOI: 10.1021/jacs.8b09247
J. Am. Chem. Soc. 2018, 140, 16206–16212

(25) Zhao, X.; et al. Mo-Terminated Edge Reconstructions in Nanoporous Molybdenum Disulfide Film. *Nano Lett.* **2018**, *18*, 482.
(26) Deng, J.; Fampiou, I.; Liu, J.; Ramasubramaniam, A.; Medhekar, N. Edge stresses of non-stoichiometric edges in two-dimensional crystals. *Appl. Phys. Lett.* **2012**, *100*, 251906.
(27) Deng, J.; Yin, Y.; Niu, H.; Ding, X.; Sun, J.; Medhekar, N. V. The Edge Stresses and Phase Transitions for Magnetic BN Zigzag Nanoribbons. *Sci. Rep.* **2017**, *7*, 7855.
(28) Girit, Ç. Ö.; Meyer, J. C.; Erni, R.; Rossell, M. D.; Kisielowski, C.; Yang, L.; Park, C.-H.; Crommie, M. F.; Cohen, M. L.; Louie, S. G.; Zettl, A. Graphene at the edge: stability and dynamics. *Science* **2009**, *323*, 1705.
(29) Ataca, C.; Şahin, H.; Aktuörk, E.; Ciraci, S. Mechanical and electronic properties of MoS_2 nanoribbons and their defects. *J. Phys. Chem. C* **2011**, *115*, 3934.
(30) Jia, X.; Hofmann, M.; Meunier, V.; Sumpter, B. G.; Campos-Delgado, J.; Romo-Herrera, J. M.; Son, H.; Hsieh, Y.-P.; Reina, A.; Kong, J.; Terrones, M.; Dresselhaus, M. S. Controlled Formation of Sharp Zigzag and Armchair Edges in Graphitic Nanoribbons. *Science* **2009**, *323*, 1701.
(31) Lucking, M. C.; Bang, J.; Terrones, H.; Sun, Y.-Y.; Zhang, S. Multivalency-Induced Band Gap Opening at MoS_2 Edges. *Chem. Mater.* **2015**, *27*, 3326.
(32) Zhou, W.; Zou, X.; Najmaei, S.; Liu, Z.; Shi, Y.; Kong, J.; Lou, J.; Ajayan, P. M.; Yakobson, B. I.; Idrobo, J.-C. Intrinsic structural defects in monolayer molybdenum disulfide. *Nano Lett.* **2013**, *13*, 2615.
(33) Chen, Q.; Li, H.; Xu, W.; Wang, S.; Sawada, H.; Allen, C. S.; Kirkland, A. I.; Grossman, J. C.; Warner, J. H. Atomically flat zigzag edges in monolayer MoS_2 by thermal annealing. *Nano Lett.* **2017**, *17*, 5502.
(34) Xu, H.; Liu, S.; Ding, Z.; Tan, S. J.; Yam, K. M.; Bao, Y.; Nai, C. T.; Ng, M.-F.; Lu, J.; Zhang, C.; Loh, K. P. Oscillating edge states in one-dimensional MoS_2 nanowires. *Nat. Commun.* **2016**, *7*, 12904.
(35) Cheng, F.; Xu, H.; Xu, W.; Zhou, P.; Martin, J.; Loh, K. P. Controlled growth of 1D $MoSe_2$ nanoribbons with spatially modulated edge states. *Nano Lett.* **2017**, *17*, 1116.
(36) Lauritsen, J. V.; Kibsgaard, J.; Helveg, S.; Topsoe, H.; Clausen, B. S.; Laegsgaard, E.; Besenbacher, F. Size-dependent structure of MoS_2 nanocrystals. *Nat. Nanotechnol.* **2007**, *2*, 53.
(37) Luxa, J.; Jankovsky, O.; Sedmidubsky, D.; Medlín, R.; Maryško, M.; Pumera, M.; Sofer, Z. Origin of exotic ferromagnetic behavior in exfoliated layered transition metal dichalcogenides MoS_2 and WS_2. *Nanoscale* **2016**, *8*, 1960.
(38) Tian, W.; Zeng, Y. C.; Zhang, Z. H. Electronic properties of graphene nanoribbons with periodically hexagonal nanoholes. *J. Appl. Phys.* **2013**, *114*, 074307.
(39) Lv, H. Y.; Lu, W. J.; Li, J. Y.; Xiao, R. C.; Wei, M. J.; Tong, P.; Zhu, X. B.; Sun, Y. P. Edge-controlled half-metallic ferromagnetism and direct-gap semiconductivity in ZrS_2 nanoribbons. *RSC Adv.* **2017**, *7*, 33408.
(40) Krainara, N.; Limtrakul, J.; Illas, F.; Bromley, S. T. Magic Numbers in a One-Dimensional Nanosystem: ZnS Single-Walled Nanotubes. *J. Phys. Chem. C* **2013**, *117*, 22908.
(41) Kresse, G.; Furthmiiller, J. Efficiency of ab-initio total energy calculations for metals and semiconductors using a plane-wave basis set. *Comput. Mater. Sci.* **1996**, *6*, 15.
(42) Perdew, J. P.; Chevary, J. A.; Vosko, S. H.; Jackson, K. A.; Pederson, M. R.; Singh, D. J.; Fiolhais, C. Atoms, molecules, solids, and surfaces: Applications of the generalized gradient approximation for exchange and correlation. *Phys. Rev. B: Condens. Matter Mater. Phys.* **1992**, *46*, 6671.
(43) Blöchl, P. E. Projector augmented-wave method. *Phys. Rev. B: Condens. Matter Mater. Phys.* **1994**, *50*, 17953.
(44) Monkhorst, H. J.; Pack, J. D. Special points for Brillouin-zone integrations. *Phys. Rev. B* **1976**, *13*, 5188.
(45) Henkelman, G.; Uberuaga, B. P.; Jónsson, H. A climbing image nudged elastic band method for finding saddle points and minimum energy paths. *J. Chem. Phys.* **2000**, *113*, 9901.

DOI: 10.1021/jacs.8b09247
J. Am. Chem. Soc. 2018, 140, 16206−16212